MPIKG Public Access
Author Manuscript

Published in final edited form as:

Pieber, B., Malik, J., Cavedon, C., Gisbertz, S., Savateev, A., Cruz, D., et al. (2019). Semi-heterogeneous dual nickel/photo-catalysis using carbon nitrides: esterification of carboxylic acids with aryl halides. Angewandte Chemie International Edition, 58(28), 9575-9580. doi:10.1002/anie.201902785.

Semi-Heterogeneous Dual Nickel/Photocatalysis using Carbon Nitrides: Esterification of Carboxylic Acids with Aryl Halides

Bartholomäus Pieber, Jamal A. Malik, Cristian Cavedon, Sebastian Gisbertz, Aleksandr Savateev, Daniel Cruz, Tobias Heil, Guigang Zhang and Peter H. Seeberger

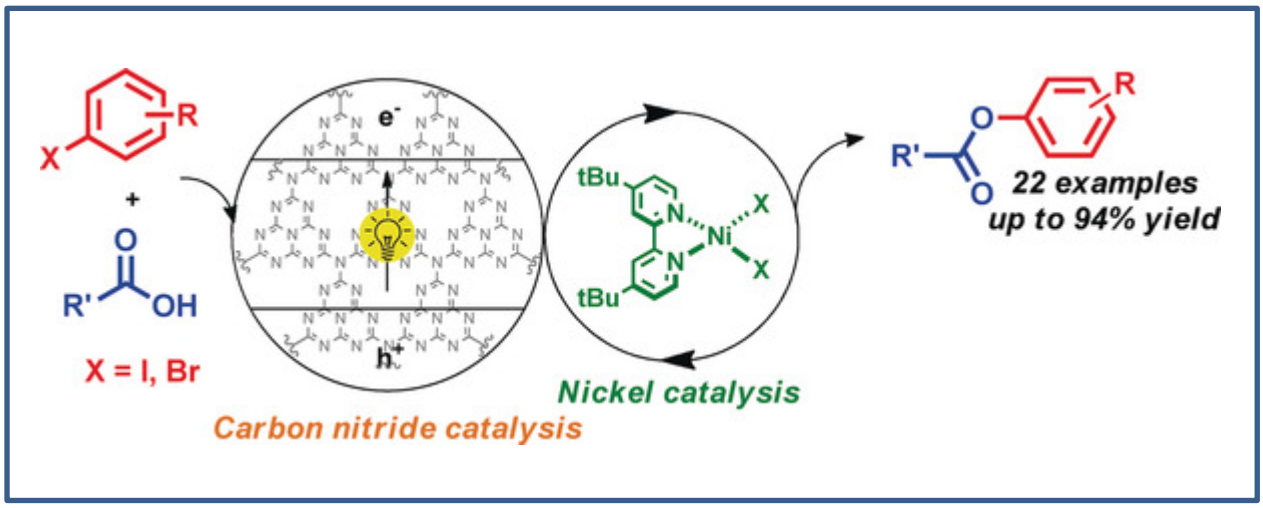

No solution necessary : A graphitic carbon nitride in combination with nickel catalysis can induce selective C–O cross-coupling. The organic semiconductor exhibits a broad substrate scope, is able to harvest green light, and can be recycled multiple times. It thus provides a sustainable alternative to the non-recyclable noble-metal complexes typically used as photocatalysts.

This article may be used for non-commercial purposes in accordance with Wiley Terms and Conditions for Self-Archiving.

Max Planck Institute of Colloids and Interfaces · Author Manuscript

Semi-Heterogeneous Dual Nickel/Photocatalysis using Carbon Nitrides: Esterification of Carboxylic Acids with Aryl Halides

Bartholomäus Pieber,[a]* Jamal A. Malik,[a] Cristian Cavedon,[a] Sebastian Gisbertz,[a] Aleksandr Savateev,[b] Daniel Cruz,[b] Tobias Heil,[b] Guigang Zhang[b] and Peter H. Seeberger[a]

Abstract: Cross-coupling reactions via dual nickel/photocatalysis are synthetically attractive but rely mainly on expensive, non-recyclable noble metal complexes as photocatalysts. Heterogeneous semiconductors, commonly used for artificial photosynthesis and wastewater treatment, are a sustainable alternative. Graphitic carbon nitrides, a class of metal-free polymers that can be easily prepared from bulk chemicals, are heterogeneous semiconductors with high potential for photocatalytic organic transformations. Here, we demonstrate that graphitic carbon nitrides in combination with nickel catalysis can induce selective C–O cross-couplings of carboxylic acids with aryl halides, yielding the respective aryl esters in excellent yield and selectivity. The organic semiconductor exhibits a broad substrate scope, is able to harvest green light, and can be recycled multiple times. *In situ* FTIR was used to track the reaction progress to study this transformation at different irradiation wavelengths and reaction scales.

Transition-metal catalyzed cross-coupling reactions are key transformations in modern organic synthesis.[1] Numerous elegant and robust methods relying primarily on palladium catalysts to form carbon–carbon[2] and carbon–heteroatom[3] bonds exist. High economic and environmental cost of precious metal catalysts renders the catalytic systems not viable in the long-term. Nickel, an attractive alternative to rare metals, is capable of catalyzing many of the same transformations as palladium.[4] The combination of nickel and photoredox catalysis opened up new avenues for cross-coupling chemistry.[5] Still, ruthenium or iridium photocatalysts (PC) are required to turn over the nickel species. Photoactive complexes with earth abundant metals[6] or organic dyes[7] are less efficient or prone to degradation.

Heterogeneous semiconductors are promising alternatives given their ease of preparation and straightforward recycling strategies by filtration or centrifugation.[8] Graphitic carbon nitrides (g-CN), a class of metal-free polymers, are among the most potent materials for heterogeneous photocatalysis.[9] Unlike the most widely studied semiconductor TiO_2 (band gap ~3.2 eV; onset of absorption: 380-390 nm), g-CN materials absorb light in the visible area (band gap <2.7 eV; onset of absorption: <450-460 nm). g-CN polymers are easy to synthesize from commodity chemicals, and exhibit a high thermal and chemical stability. The band gap and position of the valence and conduction band depend on several factors such as the C/N ratio, the polymerization degree, or the crystallinity, all of which can be tailored via the synthetic approach.[9a]

Here, we describe the application of g-CN materials in dual nickel/photocatalysis in a semi-heterogeneous catalytic system (Scheme 1).

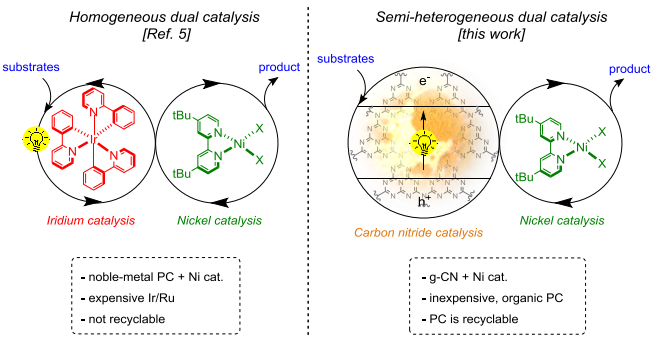

Scheme 1. Homogeneous versus semi-heterogeneous dual Ni/photocatalysis.

Carbon nitride materials can catalyze the esterification between *N*-(*tert*-Butoxycarbonyl)-proline (Boc-Pro-OH) and methyl 4-iodobenzoate using white LED (RGB) irradiation (Table 1). Mesoporous graphitic carbon nitride (mpg-CN),[10] a modified carbon nitride derived from a cyanuric acid/melamide/barbituric acid complex ($CMB_{0.05}$-CN),[11] a sulfur-doped material (CNS_{600}),[12] and the strongly oxidizing potassium poly(heptazine imide) (K-PHI),[13] gave 12-15% of ester **1**. A carbon nitride derivative prepared *via* co-condensation of urea and oxamide followed by post-calcination in a molten salt (CN-OA-m)[14] showed the highest activity in the photocatalyst screening,[15] presumably due to its enhanced optical absorption in the visible region compared to most other known CN materials (Supporting Information, Figure S1). The absence of any detectable amounts of the corresponding decarboxylative C–C coupling product **2**[16] indicates a selective photosensitization rather than single-electron transfer process.[17] This is in stark contrast to the usual reactivity of carbon nitride materials which are reported to follow single electron transfer (photoredox) pathways.[9b]

A systematic evaluation of all other reaction parameters indicated that a cocktail consisting of CN-OA-m (3.33 mg mL^{-1}), $NiCl_2$·glyme, 4,4-di-*tert*-butyl-2,2-dipyridyl (dtbbpy), and *N*-*tert*-butylisopropylamine (BIPA) in dimethyl sulfoxide (DMSO) is

[a] Dr. B. Pieber, Dr. J. A. Malik, C. Cavedon, S. Gisbertz, Prof. Dr. P. H. Seeberger
Department of Biomolecular Systems
Max-Planck-Institute of Colloids and Interfaces
Am Mühlenberg 1, 14476 Potsdam, Germany
E-mail: bartholomaeus.pieber@mpikg.mpg.de

[b] Dr. A. Savateev, D. Cruz, Dr. T. Heil, Dr. G. Zhang
Department of Colloid Chemistry
Max-Planck-Institute of Colloids and Interfaces
Am Mühlenberg 1, 14476 Potsdam, Germany

Supporting information for this article is given via a link at the end of the document

Max Planck Institute of Colloids and Interfaces · Author Manuscript

Table 1. Screening of potential carbon nitride semiconductors. [a]

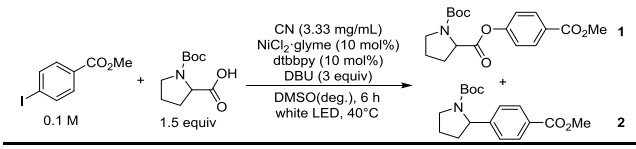

Entry	CN catalyst	1 [%][b]	2 [%][b]
1	CN-OA-m	22	n.d.[c]
2	CNS_{600}	18	n.d.
3	mpg-CN	15	n.d.
4	K-PHI	14	n.d.
5	$CMB_{0.05}$-CN	12	n.d.

[a] Reaction conditions: methyl 4-iodobenzoate (0.3 mmol), Boc-Pro-OH (0.45 mmol), $NiCl_2$·glyme (10 mol%), dtbbpy (10 mol%), 1,8-diazabicyclo[5.4.0]undec-7-ene (DBU, 0.45 mmol), CN catalyst (10 mg), DMSO (anhydrous, 3 mL), white LEDs at 40 °C for 14 h. [b] Determined by ^{1}H-NMR using 1,3,5-trimethoxybenzene as internal standard. [c] not detected.

particularly suited, obtaining the desired ester **1** in 96% after 14 h irradiation (Table 2, Entry 1).[15] The only side products were small amounts of the dehalogenated methylbenzoate **3** and the corresponding phenol **4,** which either originates from etherification with residual water[18] or ester hydrolysis. The selectivity is identical to the homogeneous protocol using $Ir(ppy)_3$ (Entry 2). Inexpensive $Ni(OAc)_2 \cdot 4H_2O$ shows similar catalytic activity (Entry 3), but an additional side product (methyl 4-acetoxybenzoate, 6%) resulted from the esterification of the aryl iodide with the acetate anion of $Ni(OAc)_2 \cdot 4H_2O$. The method also selectively converts the corresponding bromide to the desired product **1**, albeit with lower efficiency (Entry 4). Control experiments showed that the reaction does not occur in the absence of carbon nitride, nickel catalyst, or light; and just small amounts of the desired product were observed in absence of ligand (10%) or base (3%).

The synthetic versatility of the catalytic system was evaluated using both nickel catalysts (Scheme 2).[15] The anhydrous $NiCl_2$·glyme gave best results with 3 equiv of BIPA whereas inexpensive $Ni(OAc)_2 \cdot 4H_2O$ necessitated a higher excess of the base (Supporting Information, Table S7 & Figure S6). Both systems work well with electron-deficient aryl iodides (**1**, **5-15**) whereas substrates lacking an electron-withdrawing group show low reactivity (**27**, **28**). A broad range of functional groups including esters (**1**, **10**, **13**), nitriles (**5**, **14**), ketones (**6**, **15**), aldehydes (**8**), and boronic acid pinacol esters (**9**) were tolerated under the conditions applied. *Para*-substituted aryl iodides (**1**, **5, 6**) react significantly faster than their *meta* analogues (**13-15**). Although substituents in the *ortho*-position are tolerated (**10**), low reactivity for 2-iodobenzonitrile (**26**) was observed. Carbonyl groups in the 2-position (**31**, **33**) do not give the corresponding ester product. We assume that, after the initial oxidative addition of the aryl halide, coordination of the carbonyl oxygen to the metal center[19] hinders association of the carboxylate

Table 2. Optimized conditions and control experiments[a]

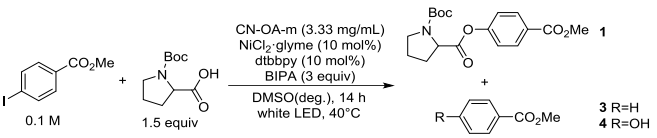

Entry	Conditions	1 [%][b]	3 [%][b]	4 [%][b]
1	as shown	96	trace	2
2	$Ir(ppy)_3$ (1mol%) instead of CN-OA-m	97	trace	1
3	$Ni(OAc) \cdot 4H_2O$ instead of $NiCl_2$·glyme[c]	85	trace	4
4	4-Methyl bromobenzoate as substrate	68	5	2
5	No CN-OA-m	n.d.[c]	n.d.	n.d.
6	No $NiCl_2$·glyme	n.d.	2	1
7	No dtbbpy	10	3	2
8	No light	n.d.	n.d.	n.d.
9	No base	3	trace	n.d.

[a] Reaction conditions: methyl 4-iodobenzoate (0.3 mmol), Boc-Pro-OH (0.45 mmol), $NiCl_2$·glyme (10 mol%), dtbbpy (10 mol%), BIPA (0.9 mmol), CN-OA-m (10 mg), DMSO (anhydrous, 3 mL), white LEDs at 40 °C for 14 h. [b] Determined by ^{1}H-NMR using 1,3,5-trimethoxybenzene as internal standard. [c] 5 equiv BIPA were used. [d] not detected.

nucleophile. 1-Bromo-4-iodobenzene gave the desired product **11** without any detectable amount of the 1,4-diester, as the iodo-group reacts significantly faster and the resulting esterification product deactivates the aryl bromide towards a second esterification. With respect to the carboxylic acid coupling partner, a wide array of substrates can be efficiently coupled, including aliphatic (**16**, **19**, **21**, **22**), olefinic (**17**), and benzylic (**20**, **24**) carboxylic acids, as well as benzoic acid derivatives (**18**, **23**). The esterification of Biotin (**25**) shows the potential of the presented methodology for conjugation purposes. Artesunate (**35**), acetylated sialic acid (**36**) as well as the unprotected amine **34** did not give the desired ester under these reaction conditions. In all cases, $NiCl_2$·glyme resulted in a significantly higher selectivity than $Ni(OAc)_2 \cdot 4H_2O$ partly due to coupling of the acetate anion with the aryl iodide (up to 22%) and partly from the formation of higher quantities of the dehalogenated and phenol side products (Supporting Information, Table S14 & S15).

A major advantage of carbon nitride catalysis is the potential to reuse the heterogeneous material.[20] With dual nickel/carbon nitride catalysis, however, deposition of Ni on the semiconducting material is possible and may alter its photocatalytic properties.[9a] As such, we sought to determine whether the CN-OA-m material is recyclable in our catalytic system (Figure 1). CN-OA-m was recovered after each reaction by centrifugation, washed, and used in the next reaction by adding fresh $NiCl_2$·glyme and dtbbpy. The material proved to be

Max Planck Institute of Colloids and Interfaces · Author Manuscript

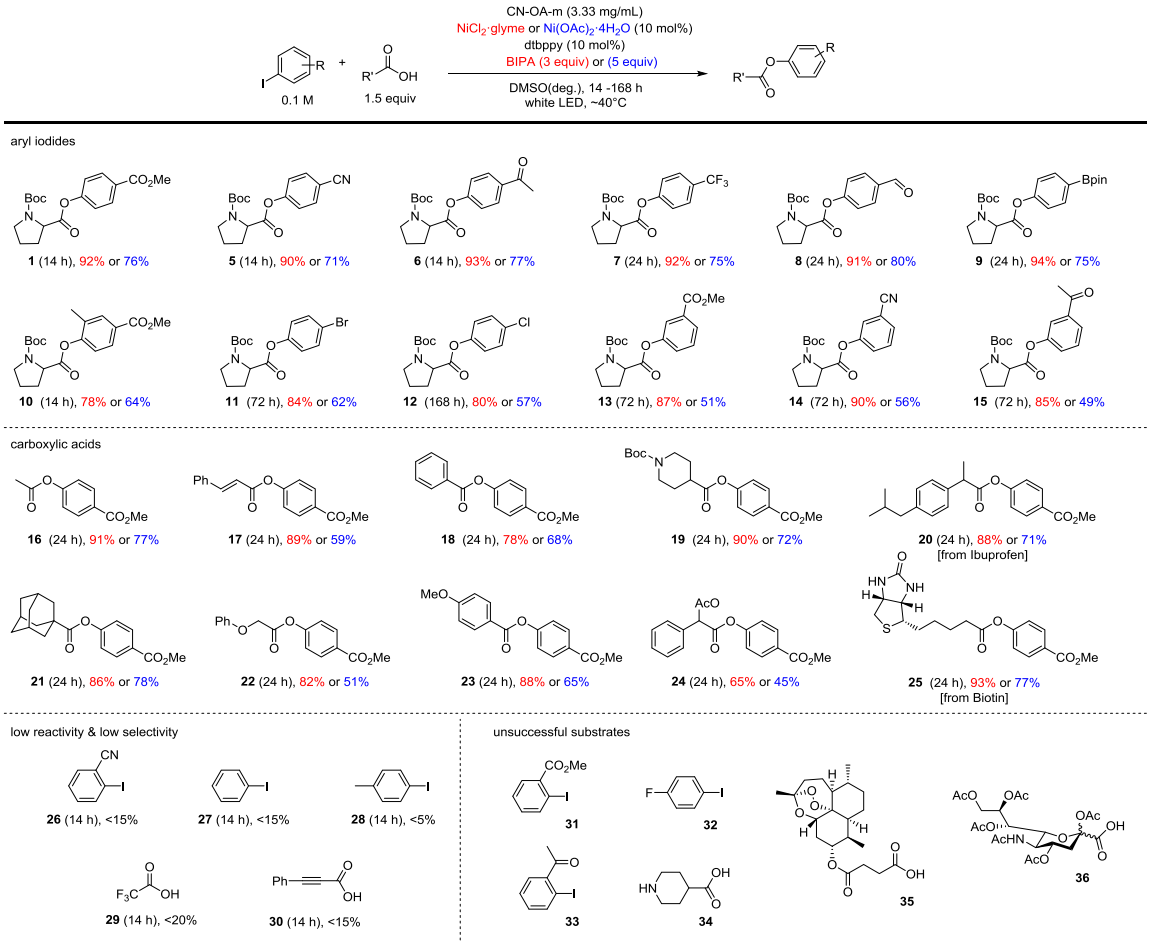

Scheme 2. Scope of the semi-heterogeneous esterification of carboxylic acids with aryl iodides.

reusable without any loss of the catalytic activity over three cycles. Thereafter, a reduction in the yield of **1** from 96 to ~80% was noticed. This may result from a reduced availability of active catalytic sites for the photocatalytic step due to deposited Ni species,[15] but could be also rationalized by the loss of small amounts of the photocatalyst during the series of experiments. Analysis of the heterogeneous catalyst before and after a reaction using X-ray powder diffraction (XRD) showed the same characteristic peaks at 8° and 28° for CN-OA-m without any obvious Ni species in case of the recovered semiconductor (Figure 2, A). Similarly, identical FTIR (Figure 2, B) and UV/Vis spectra (Figure 2, C) were observed for the recovered and fresh CN-OA-m catalyst, proofing that the photocatalytic properties are not changing. The morphology of CN-OA-m shows a porous texture that was not altered during the catalytic transformation (Figure 2, E & F). As highly dispersed Ni species are potentially undetectable by XRD,[21] X-ray photoelectron spectroscopy (XPS) detected Ni in the recovered material (Figure 2, D). The high resolution XPS Ni2 $p_{3/2}$ spectrum of the recovered CN-OA-m material shows two main deconvoluted peaks located at 853.7(±0.02) eV and 852.5 (±0.02) eV that can be assigned to the binding energy of Ni^{2+} and Ni^{0} species, respectively (Supporting Information, Figure S13). Nickel deposition was further confirmed by ICP-OES analysis showing a Ni

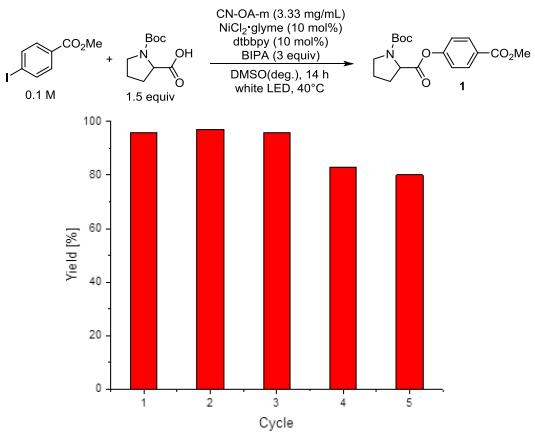

Figure 1. Reusability of CN-OA-m in the dual nickel/photocatalytic esterification of methyl 4-iodobenzoate with Boc-Pro-OH.

Max Planck Institute of Colloids and Interfaces · Author Manuscript

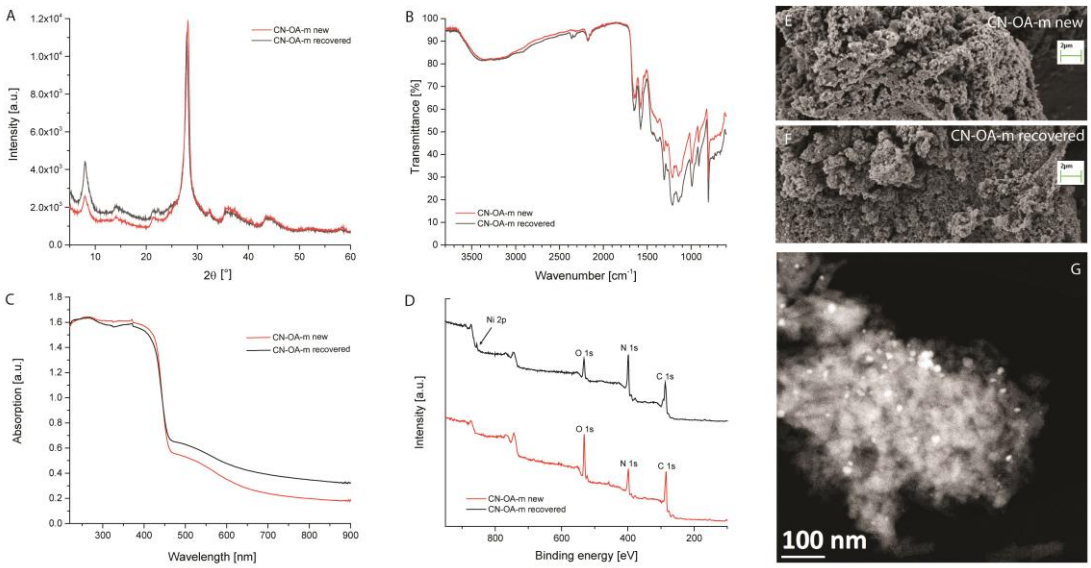

Figure 2. Analysis of new and recovered CN-OA-m by powder XRD (A), FTIR (B), UV/Vis (C) and XPS (D) spectroscopy as well as SEM analysis (E & F). HAADF-STEM image (G) of nickel particles (bright spots) attached to the recovered CN-OA-m.

concentration of 1.4 % w/w suggesting that 5-8% of the homogeneous nickel catalyst was deposited on the organic semiconductor.[15] Scanning transmission electron microscopy (STEM) was used to visualize nickel particles on the surface of the recovered CN-OA-m (Figure 2, G).

To determine whether the immobilized nickel is catalytically active in the model reaction, the esterification was carried out with the recovered CN-OA-m material from one and five reaction cycles in the absence of additional $NiCl_2$·glyme. Both experiments resulted in no more than ~6% ester **1**, clearly indicating that the adsorbed, low-valent Ni species do not serve as effective catalytic species.[15]

To study the scalability of the photocatalytic system and to determine if the photocatalytic system can harvest energy from varying light sources, a real-time monitoring strategy was developed.[15] Although NMR is often an ideal choice for kinetic analysis and has been used to track photocatalytic transformations,[22] the presence of a heterogeneous component that broadens peaks, and the potential involvement of paramagnetic nickel species precluded its use. *In situ* FTIR analysis eliminates any interference from the heterogeneous photocatalyst,[23] and provides high-fidelity reaction tracking under normal reaction conditions. Observing the reaction under optimized reaction conditions, an incipient peak at ~1764 cm^{-1} (Figure 3, A), separable from the other two carbonyl stretches in the reaction mixture, was observed. This C=O stretch from the product's internal ester is heavily blue-shifted from the corresponding acid starting material. This peak served as a competent measure of reaction progress (Supporting Information, Figure S8).

After a brief induction period, the catalysis reaches its maximum rate quickly and proceeds until completion (Figure 3B, black). A highly similar kinetic profile was observed using $Ir(ppy)_3$ (Figure 3B, grey), showcasing that the heterogeneous catalyst has not only the same selectivity (Table 2) but also comparable efficiency with the state-of-the-art homogeneous noble metal photocatalysts. Although slower than the aryl iodide, the bromide (Figure 3B, purple) furnished the product in 88% yield within 48 h (Supporting Information, Figure S9). Scale-up of the esterification from 0.3 mmol to 3.0 mmol (Figure 3B, orange) is facile, affording the desired ester **1** in 96% isolated yield on gram scale in roughly six instead of three hours using this setup. As this scaled-up reaction has the same concentration of all components, the longer reaction time is mostly due to Beer–Lambert limitations inherent in using a larger reaction vessel (Supporting Information, Figure S8).

The *in situ* method was also employed to assess the reaction's progress with different light settings from the same LED strips (Figure 3, C). Blue light (~400 – 500 nm) catalyzes the reaction to completion, albeit slower, as the energy from light above 500 nm is not available (Supporting Information, Figure S3). Red light (600 – 650 nm), and a control experiment in the dark, afforded no meaningful amount of product. Encouragingly, green light (460 – 600 nm) begets partial completion in an overnight reaction, affirming that the heterogeneous photocatalyst is able to use a wide spectrum of visible light (Supporting Information, Figure S1). After eight days, the reaction gave 72% **1** (Supporting Information, Figure S12).

In conclusion, it was shown that a homogeneous nickel catalyst can be combined with a heterogeneous, metal-free carbon nitride semiconductor for dual catalysis. The insoluble photocatalyst can be recycled multiple times. Two nickel catalysts were studied in detail for a broad range of substrates, with $NiCl_2$·glyme showing a significantly higher selectivity than $Ni(OAc)_2{\cdot}4H_2O$, which nonetheless resulted in moderate to good yields of the desired esters. The organic semiconductor is able

Max Planck Institute of Colloids and Interfaces · Author Manuscript

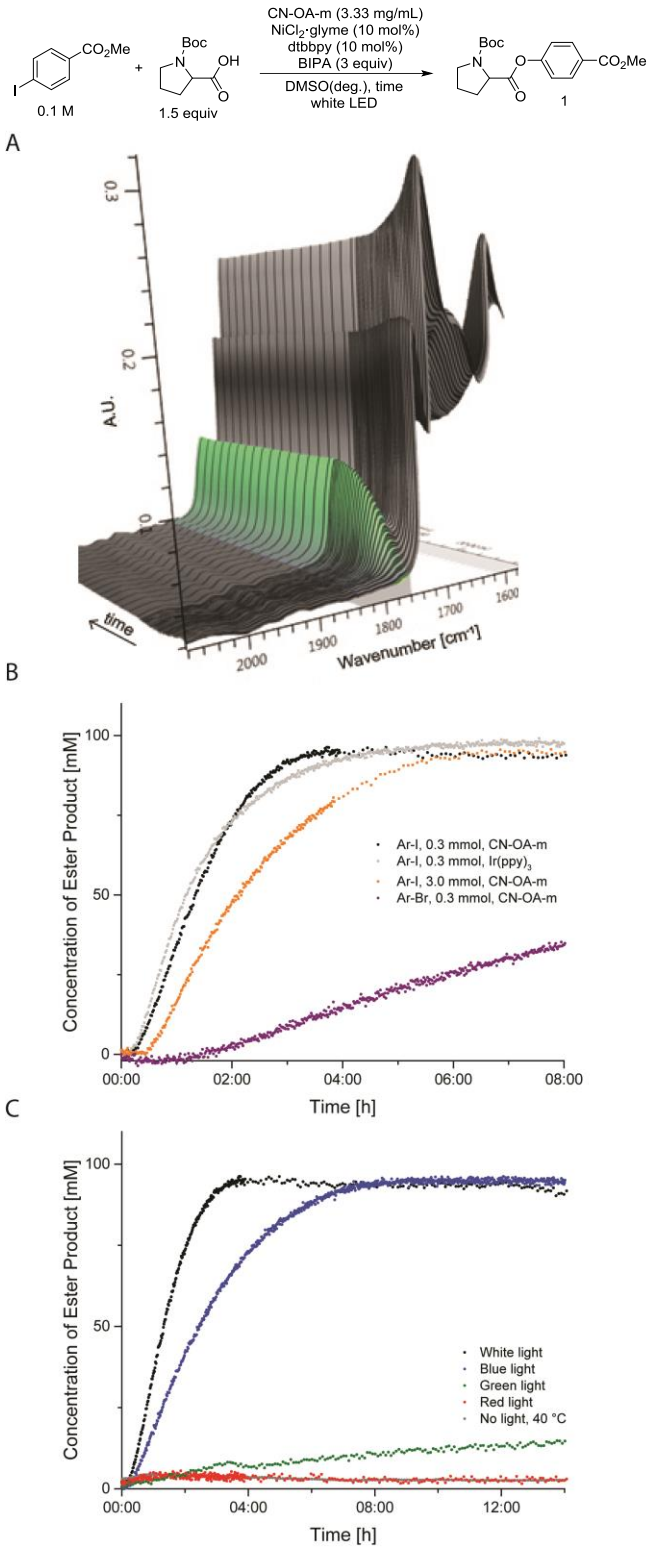

Figure 3. *In situ* reaction tracking of dual catalytic esterification. A, The internal ester peak at ~1764 cm^{-1} serves as a measure of reaction progress. B, Small-scale (0.3 mmol substrate) with the aryl iodide (black) and bromide (purple) as well as a gram-scale reaction (3.0 mmol methyl 4-iodobenzoate, orange) were easily tracked *in situ*. A comparison with $Ir(ppy)_3$ as PC shows a similar kinetic profile (grey). C, White light (black) and blue light (blue) catalyze the reactions quickly, while green light (green) also shows activity.

to harvest a broad range of the visible light spectrum (up to ~600 nm) as shown by *in situ* FTIR analysis. The FTIR reaction monitoring strategy was used, to the best of our knowledge, for the first time to study photocatalytic transformations and is essential to analyze reaction progress kinetics of photocatalysis to better understand the underlying mechanisms. The inexpensive heterogeneous materials are an efficient and sustainable alternative to noble-metal complexes in photocatalysis.

Acknowledgements

We gratefully acknowledge the Max-Planck Society for generous financial support. B.P. acknowledges financial support by a Liebig Fellowship of the German Chemical Industry Fund (Fonds der Chemischen Industrie, FCI). S.G. and B.P. acknowledge the International Max Planck Research School on Multiscale Bio-Systems for financial support. We thank our colleagues Markus Antonietti, Martin Oschatz, Tobias Schmidt, Cliff Janiszewski, Rona Pitschke, Heike Runge, Katharina Otte (all MPIKG), Matthew Mower (Janssen Pharmaceutical), and Dario Cambié (Eindhoven University of Technology) for scientific, technical and analytical support.

Keywords: graphitic carbon nitride • photocatalysis • heterogeneous catalysis • metallaphotoredox • dual catalysis

[1] R. H. Crabtree, *The organometallic chemistry of the transition metals*, John Wiley & Sons, **2009**.
[2] C. C. C. Johansson Seechurn, M. O. Kitching, T. J. Colacot, V. Snieckus, *Angew. Chem. Int. Ed.* **2012**, *51*, 5062.
[3] J. F. Hartwig, *Nature* **2008**, *455*, 314.
[4] a) S. Z. Tasker, E. A. Standley, T. F. Jamison, *Nature* **2014**, *509*, 299; b) B. M. Rosen, K. W. Quasdorf, D. A. Wilson, N. Zhang, A.-M. Resmerita, N. K. Garg, V. Percec, *Chem. Rev.* **2011**, *111*, 1346; c) V. P. Ananikov, *ACS Catal.* **2015**, *5*, 1964.
[5] a) J. Twilton, C. Le, P. Zhang, M. H. Shaw, R. W. Evans, D. W. C. MacMillan, *Nat. Rev. Chem.* **2017**, *1*, 0052; b) G. Molander, J. A. Milligan, J. P. Phelan, S. O. Badir, *Angew. Chem. Int. Ed.* **2019**, doi:10.1002/anie.201809431.
[6] O. S. Wenger, *J. Am. Chem. Soc.* **2018**, *140*, 13522.
[7] a) N. A. Romero, D. A. Nicewicz, *Chem. Rev.* **2016**, *116*, 10075; b) C. Lévêque, L. Chenneberg, V. Corcé, C. Ollivier, L. Fensterbank, *Chem. Commun.* **2016**, *52*, 9877; c) Y. Du, R. M. Pearson, C.-H. Lim, S. M. Sartor, M. D. Ryan, H. Yang, N. H. Damrauer, G. M. Miyake, *Chem. Eur. J.* **2017**, *23*, 10962; d) C. Fischer, C. Sparr, *Angew. Chem. Int. Ed.* **2018**, *57*, 2436.
[8] a) D. Friedmann, A. Hakki, H. Kim, W. Choi, D. Bahnemann, *Green Chem.* **2016**, *18*, 5391; b) X. Lang, X. Chen, J. Zhao, *Chem. Soc. Rev.* **2014**, *43*, 473; c) J. Chen, J. Cen, X. Xu, X. Li, *Catal. Sci. Technol.* **2016**, *6*, 349.
[9] a) W.-J. Ong, L.-L. Tan, Y. H. Ng, S.-T. Yong, S.-P. Chai, *Chem. Rev.* **2016**, *116*, 7159; b) A. Savateev, I. Ghosh, B. König, M. Antonietti, *Angew. Chem. Int. Ed.* **2018**, *57*, 15936.
[10] F. Goettmann, A. Fischer, M. Antonietti, A. Thomas, *Angew. Chem. Int. Ed.* **2006**, *45*, 4467.
[11] M. Shalom, M. Guttentag, C. Fettkenhauer, S. Inal, D. Neher, A. Llobet, M. Antonietti, *Chem. Mater.* **2014**, *26*, 5812.
[12] J. Zhang, J. Sun, K. Maeda, K. Domen, P. Liu, M. Antonietti, X. Fu, X. Wang, *Energy Environ. Sci.* **2011**, *4*, 675.
[13] A. Savateev, S. Pronkin, J. D. Epping, M. G. Willinger, C. Wolff, D. Neher, M. Antonietti, D. Dontsova, *ChemCatChem* **2017**, *9*, 167.
[14] G. Zhang, G. Li, Z.-A. Lan, L. Lin, A. Savateev, T. Heil, S. Zafeiratos, X. Wang, M. Antonietti, *Angew. Chem. Int. Ed.* **2017**, *56*, 13445.
[15] See Supporting information for details.
[16] Z. Zuo, D. T. Ahneman, L. Chu, J. A. Terrett, A. G. Doyle, D. W. C. MacMillan, *Science* **2014**, *345*, 437.

Max Planck Institute of Colloids and Interfaces · Author Manuscript

[17] E. R. Welin, C. Le, D. M. Arias-Rotondo, J. K. McCusker, D. W. C. MacMillan, *Science* **2017**, *355*, 380.
[18] a) J. A. Terrett, J. D. Cuthbertson, V. W. Shurtleff, D. W. C. MacMillan, *Nature* **2015**, *524*, 330; b) L. Yang, Z. Huang, G. Li, W. Zhang, R. Cao, C. Wang, J. Xiao, D. Xue, *Angew. Chem. Int. Ed.* **2018**, *57*, 1968.
[19] J. Cámpora, I. Matas, C. M. Maya, P. Palma, E. Álvarez, *Organometallics* **2006**, *25*, 3124.
[20] B. Pieber, M. Shalom, M. Antonietti, P. H. Seeberger, K. Gilmore, *Angew. Chem. Int. Ed.* **2018**, *57*, 9976.
[21] H. B. Yang, S.-F. Hung, S. Liu, K. Yuan, S. Miao, L. Zhang, X. Huang, H.-Y. Wang, W. Cai, R. Chen, J. Gao, X. Yang, W. Chen, Y. Huang, H. M. Chen, C. M. Li, T. Zhang, B. Liu, *Nat. Energy* **2018**, *3*, 140.
[22] C. Feldmeier, H. Bartling, E. Riedle, R. M. Gschwind, *J. Magn. Reson.* **2013**, *232*, 39.
[23] a) T. C. Malig, J. D. B. Koenig, H. Situ, N. K. Chehal, P. G. Hultin, J. E. Hein, *React. Chem. Eng.* **2017**, *2*, 309; b) F. Sheng, P. S. Chow, Z. Q. Yu, R. B. H. Tan, *Org. Process Res. Dev.* **2016**, *20*, 1068.